

Dhofar 287

Unbrecciated basalt (with basaltic breccia)

154 g



Figure 1: Cut slab of Dhofar 287 showing the mare basalt lithology (lower reddish portion) and the regolith breccia (upper black area). Scale at bottom has smallest divisions of mm.

Introduction

Dhofar 287 (Fig. 1) was found in the Dhofar region of Oman (Figs. 2 and 3) on January 14, 2001. The 154 g dark gray stone lacks fusion crust, is strongly shocked, and contains terrestrial weathering features such as iron staining, oxidation, and carbonate veins. The sample consists of two different lithologies – unbrecciated mare basalt comprising about 95% of the rock and regolith breccia comprising the remaining 5%.

Petrography

Lithology A contains 20.6% olivine phenocrysts (1 to 2 mm) and lesser pyroxene phenocrysts (< 0.5 mm), both of which are zoned (Fig. 4). The phenocrysts are in a fine grained matrix of pyroxene, plagioclase, and accessory ilmenite, chromite, ulvospinel, troilite, FeNi metal, and a late stage mesostasis consisting of fayalite, Si-K-Ba-rich glass (Fig. 5), apatite and merrillite. The plagioclase in Dho 287A is almost entirely converted to maskelynite. The late stage mesostasis is unusually abundant compared to many other

mare basalts from the Apollo collection. Lithology B is a regolith breccia containing both lithic clasts

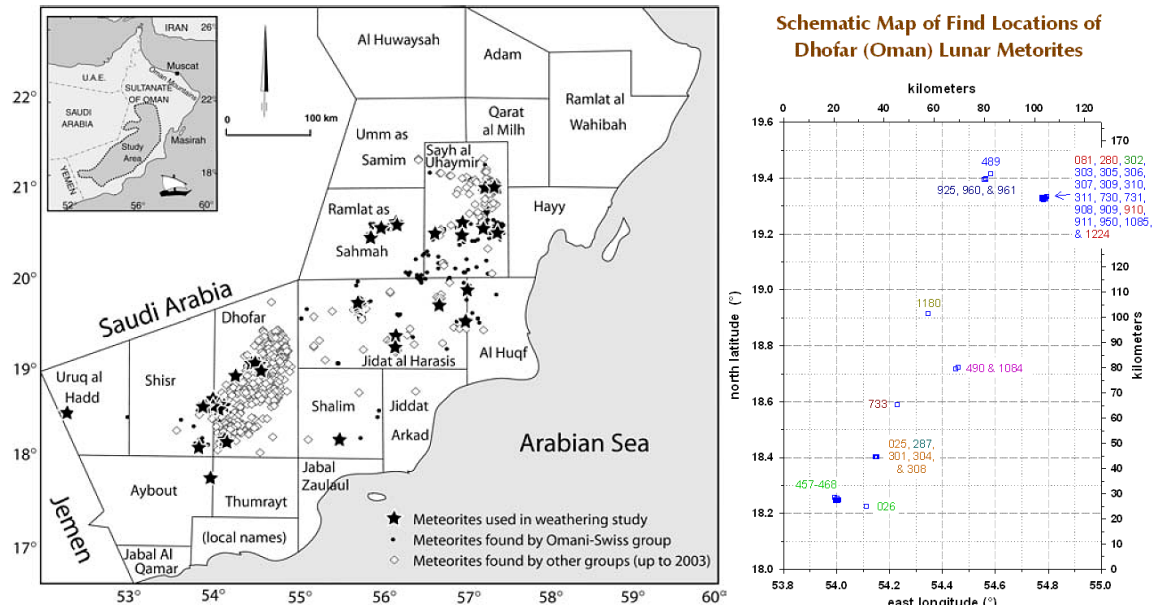


Figure 2: Map showing location of regions within Oman where meteorites have been recovered, such as Dhofar.

Figure 3: More detailed locations of the Dhofar meteorites, including Dho 287.

(~18%) and mineral fragments, most of which are basaltic in nature, in a fragmental fine grained matrix with minor impact melt. The lithic clasts are crystalline rocks (low Ti basalt, very low Ti basalt, and picritic basalt), vitrophyric rocks (pyroxene phryic basalt), and impact melt breccias (Demidova et al., 2003).

Mineralogy

Olivine phenocrysts in Dho 287A range on composition from approximately Fo₅₀ rims to Fo₇₀ cores (Fig. 6). Comparison of pyroxene compositions in Dho 287A and mineral fragments and lithic clasts in Dho 287B (Fig. 7) indicate that the similar compositional range is consistent with derivation of the breccia (B) from basaltic lithologies (A) (Demidova et al., 2003; Anand et al., 2003). Plagioclase varies in composition from An₈₅ to An₇₂, more sodic than other Apollo 12 and 15 basalts and also NWA 032 (Fig. 8). Chromite cores are rimmed with ulvospinel in Dho287A, exhibiting a large range within Cr-Al-Ti compositional space (Fig. 9).



Figure 4: cut face of Dho 287 illustrating the texture of lithology A (from R. Korotev).

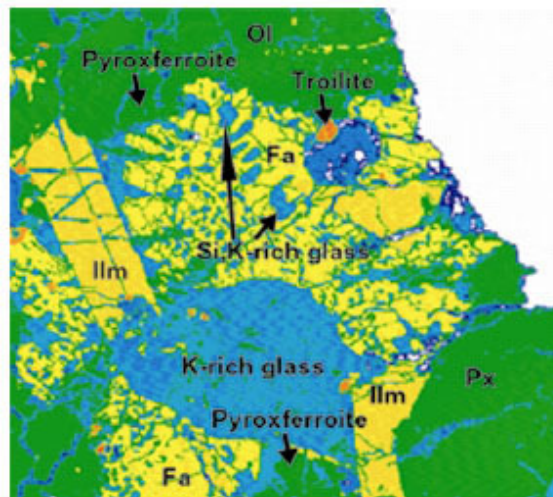


Figure 5: X-ray map of mesostasis region with pyroxferroite, K-rich glass, Si- and K-rich glass, and fayalite.

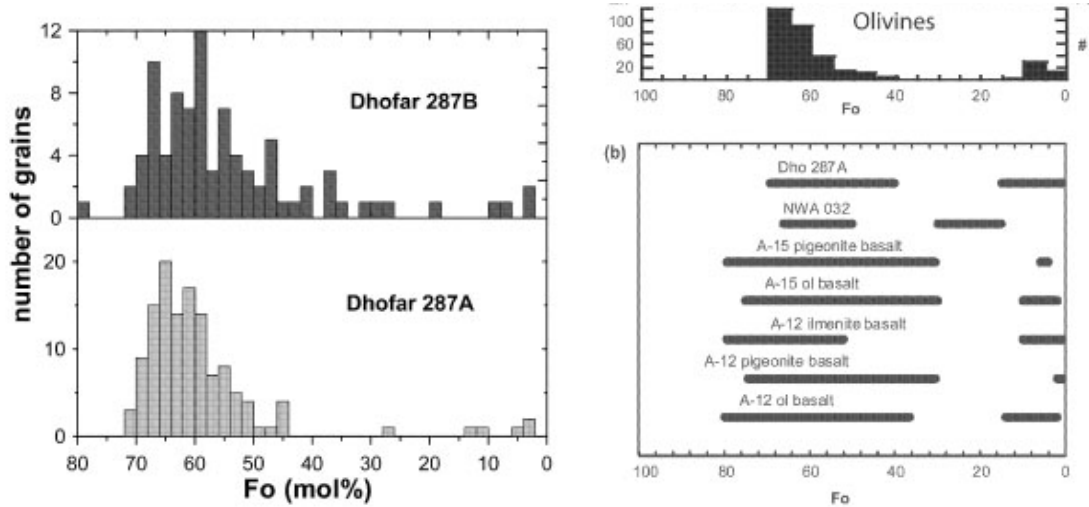


Figure 6: Olivine phenocrysts from Dho 287A compared to olivine mineral fragments in Dho 287B. Compositions overlap considerably, and also exhibit a similar range to olivine found in NWA 032 and Apollo 12 and 15 basalts (Anand et al., 2003; Demidova et al., 2003).

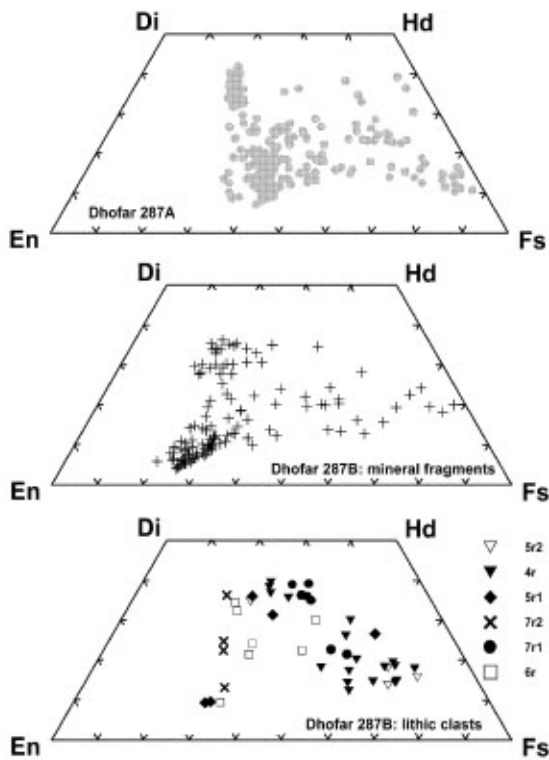


Figure 7: Pyroxene compositions in Dho 287A (top) compared to mineral fragments and lithic clasts in Dho 287B. The similar compositional range is consistent with derivation of the breccia from basaltic lithologies such as A (Demidova et al., 2003; Anand et al., 2003).

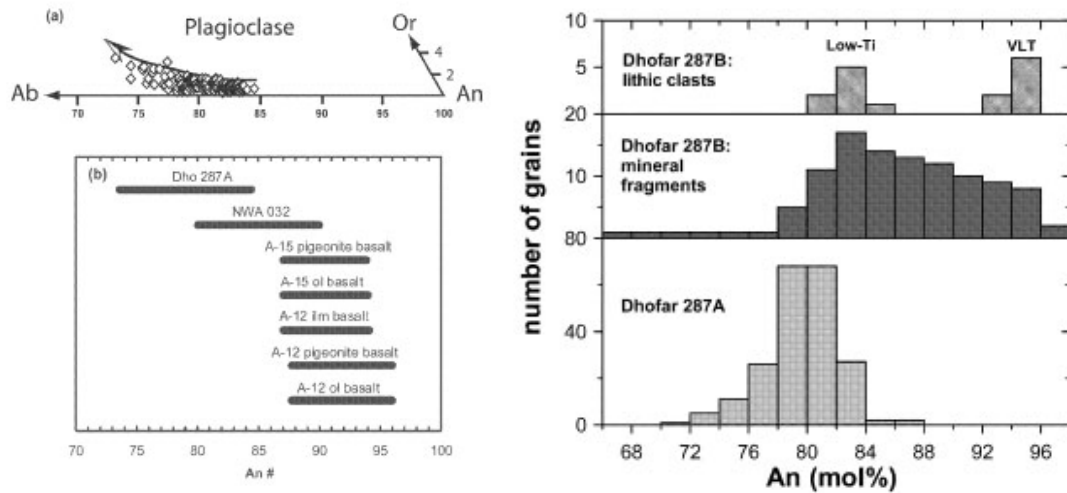


Figure 8: Plagioclase feldspar compositions in Dho 287A (top left) compared to those in NWA 032 and Apollo 12 and 15 basalts. Plagioclase compositions in mineral fragments and lithic clasts in lithology B overlap but also extend out to higher An contents (from Anand et al., 2003; Demidova et al., 2003).

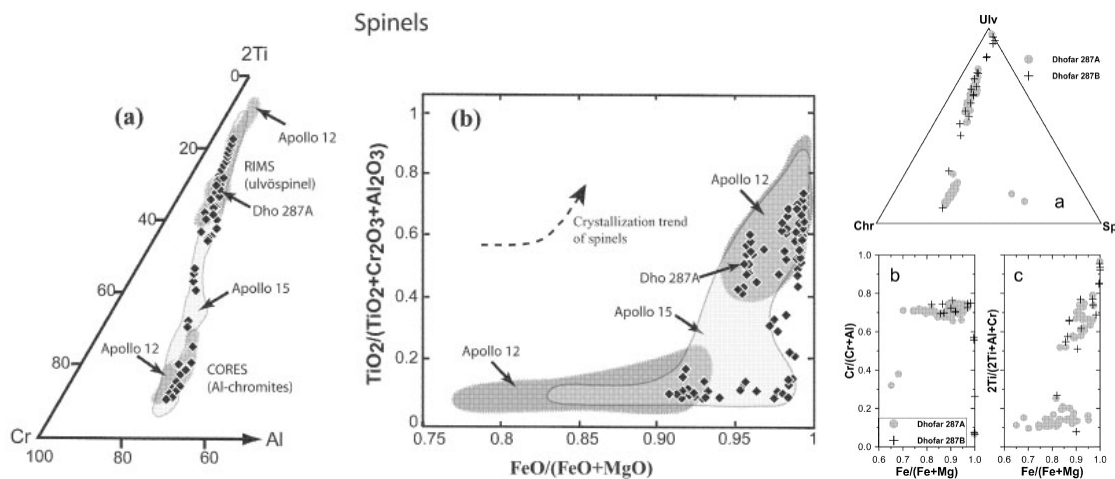


Figure 9: Spinel compositions in Dho 287A (top and grey circles in bottom) compared to mineral fragments and lithic clasts in lithology B (crosses in bottom). Lithology A spinels span a large compositional range that is similar to ranges documented in Apollo 12 and 15 basalts (Anand et al., 2003; Demidova et al., 2003).

Chemistry

Small splits of lithology A and B have been analyzed (Table 1), illuminating the magnesian composition of Dho 287A. In fact, comparison to Apollo 12 and 15 basalts show that Dho 287A falls in the low Al_2O_3 , high MgO and FeO end of the compositional spectrum defined by low Ti basalt (Fig. 10). Although this may suggest a primitive liquid, the high MgO contents (13.2 wt%) are directly attributable to the high modal olivine content (~21%). Consideration of olivine-liquid Mg-Fe equilibrium demonstrates that the olivine cores are not in equilibrium with the bulk composition, and thus that there has been olivine accumulation.

Although Dho 287A has similar REE concentrations to the Apollo 12 and 15 basalts, it is slightly elevated, which led Anand et al. (2003) to conclude that the parental liquid had assimilated as much as 8% of KREEP component (Fig. 11). Detailed modelling shows that a single composition cannot account for all of the clasts types found in lithology B. Rather, at

least three different but low Ti, compositions may be necessary to account for the variation (Fig. 12; Demidova et al., 2003).

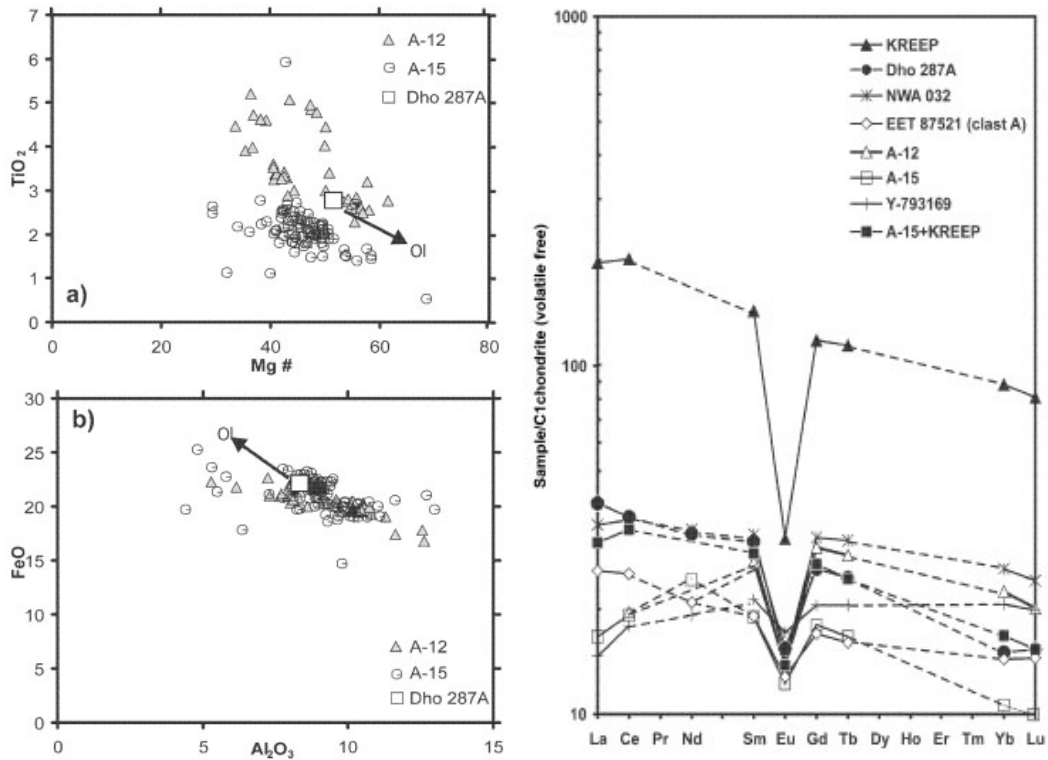


Figure 10: Major element composition of Dho 287A compared to Apollo 12 and 15 basalts.

Figure 11: REE concentrations for Dho 287A compared to those for Apollo 12 and 15 basalts as well as KREEP (from Anand et al., 2003).

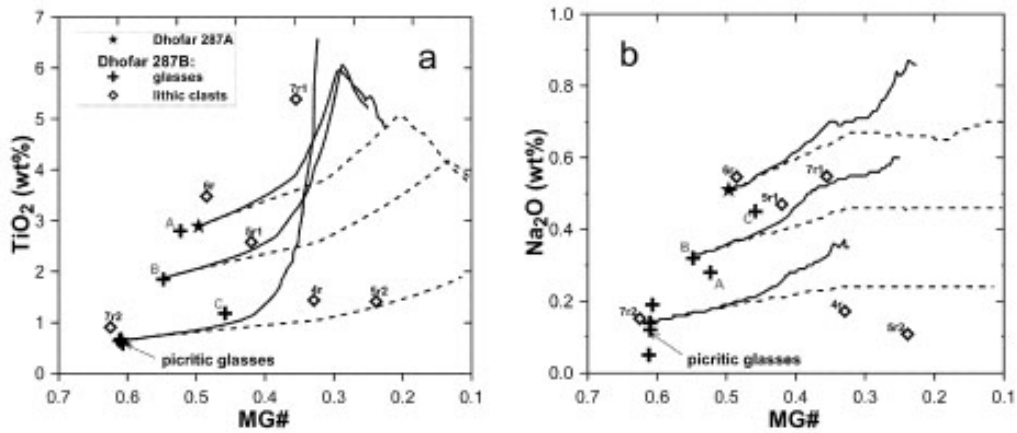


Figure 12: Ti-Na-Mg# relations for Dho 287A bulk and clasts from 287B showing their relation to modelled liquid lines of descent (solid). Several parental liquids are required to explain the entire range of clasts types (from Demidova et al., 2003).

Radiogenic age dating

Age dating using mineral separates and the Rb-Sr and Sm-Nd isotopic systems leads to a result of 3.46 Ga (Fig. 13). Additional modelling of these two systems led Shih et al. (2002) to

conclude that Dho 287A was derived from a mantle source similar to the Apollo 15 green glass, but was also affected by a minor KREEP component (Fig 14).

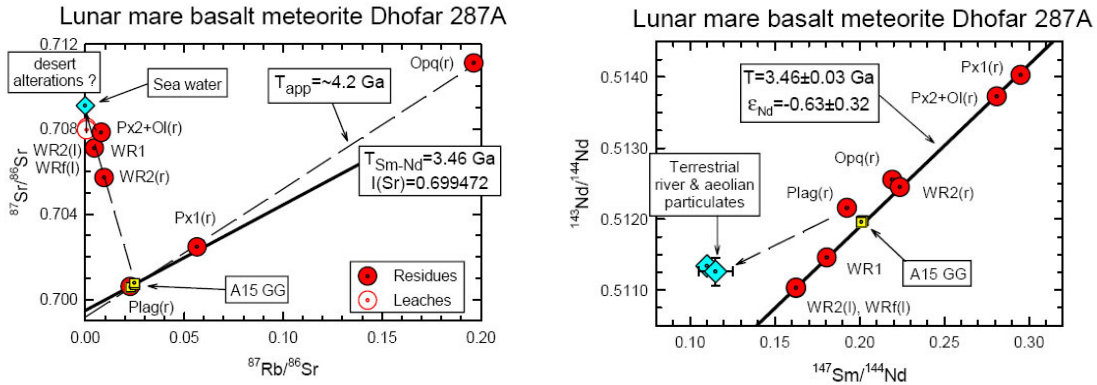


Figure 13: Mineral isochrons for Dho 287A for the Rb-Sr (left) and Sm-Nd (right) systems (from Shih et al., 2002).

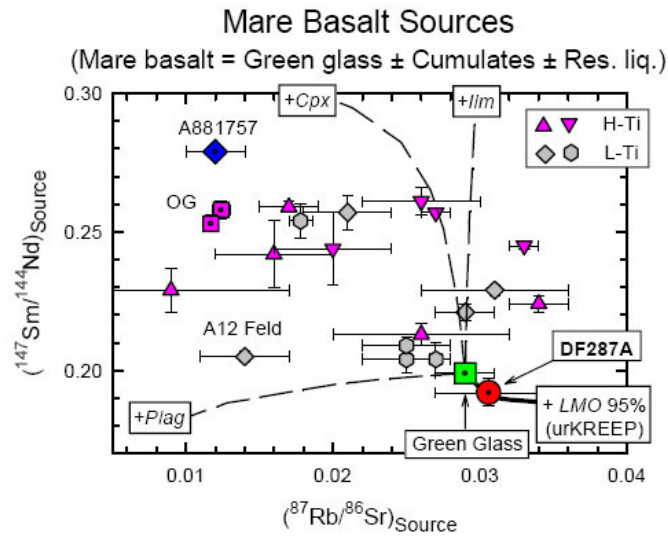


Figure 14: Calculated Sm/Nd and Rb/Sr values for the source of Dho 287A compared to other Apollo basalts, the Green Glass. Also shown are trajectories for specific minerals – ilmenite, clinopyroxene, plagioclase and urKREEP.

Cosmogenic isotopes and exposure ages

No work has been reported yet.

Table 1a. Chemical composition of Dhofar 287

| <i>reference</i> | 1 | 2 | 2 | 2 | 2 | 2 | 2 | 2 | 2 | 2 | 2 | 2 | 2 | 2 |
|--------------------------------|---------|------|------|------|-------|------|------|------|------|------|------|-------|------|------|
| <i>weight</i> | ~ 1 g | A | B | 6r | 7r1 | 5r1 | 5r2 | 4r | C | | | | | |
| <i>method</i> | b,e,f,g | d | d | d | d | d | d | d | d | d | d | d | d | d |
| SiO ₂ % | 43.2 | 44.7 | 46.6 | 46.6 | 45.5 | 47.9 | 45.8 | 46.2 | 47.7 | 46.3 | 49.8 | 44.4 | 45.7 | 44.6 |
| TiO ₂ | 2.76 | 2.8 | 1.85 | 3.48 | 5.39 | 2.58 | 1.41 | 1.44 | 1.18 | 1.84 | 4.12 | 2.15 | 3.32 | 0.64 |
| Al ₂ O ₃ | 8.35 | 7.82 | 7.77 | 11.5 | 10.7 | 10.1 | 6.14 | 10.1 | 12.3 | 17.5 | 9.85 | 12.4 | 9.49 | 6.75 |
| FeO | 22.1 | 21.5 | 19.3 | 15.3 | 18.28 | 19.6 | 29.8 | 21.6 | 17.4 | 10.5 | 15.6 | 16.52 | 20 | 20.9 |
| MnO | 0.29 | 0.28 | 0.28 | 0.2 | 0.28 | 0.28 | 0.31 | 0.29 | 0.24 | 0.17 | 0.23 | 0.2 | 0.3 | 0.29 |
| MgO | 13.2 | 13.2 | 13.1 | 8.07 | 5.65 | 7.98 | 5.24 | 5.95 | 8.25 | 9.32 | 6.21 | 10.5 | 8.68 | 18.3 |
| CaO | 8.74 | 8.53 | 8.79 | 11.7 | 13 | 9.86 | 9.65 | 12.7 | 10.6 | 11.5 | 8.84 | 10.2 | 10.1 | 7.31 |
| Na ₂ O | 0.53 | 0.28 | 0.32 | 0.55 | 0.55 | 0.47 | 0.11 | 0.17 | 0.45 | 0.64 | 0.91 | 0.48 | 0.46 | 0.14 |
| K ₂ O | 0.19 | 0.05 | 0.1 | 0.07 | 0.07 | 0.09 | 0.01 | 0.02 | 0.15 | 0.47 | 0.96 | 0.18 | 0.1 | 0.04 |
| P ₂ O ₅ | 0.21 | 0.13 | 0.11 | | | 0.09 | | | 0.2 | 0.4 | 1.24 | 0.21 | 0.22 | 0.04 |
| S % | | | | | | | | | | | | | | |
| <i>sum</i> | | | | | | | | | | | | | | |
| Sc ppm | 35.2 | | | | | | | | | | | | | |
| V | | | | | | | | | | | | | | |
| Cr | 4447 | 3421 | 5542 | 2874 | 958 | 3284 | 753 | 1163 | 2395 | 1232 | 1711 | 2668 | 2874 | 3626 |
| Co | 42.3 | | | | | | | | | | | | | |
| Ni | 20 | | | | | | | | | | | | | |
| Cu | | | | | | | | | | | | | | |
| Zn | | | | | | | | | | | | | | |
| Ga | | | | | | | | | | | | | | |
| Ge | | | | | | | | | | | | | | |
| As | | | | | | | | | | | | | | |
| Se | | | | | | | | | | | | | | |
| Rb | | | | | | | | | | | | | | |
| Sr | 530 | | | | | | | | | | | | | |
| Y | | | | | | | | | | | | | | |
| Zr | 60 | | | | | | | | | | | | | |
| Nb | | | | | | | | | | | | | | |
| Mo | | | | | | | | | | | | | | |
| Ru | | | | | | | | | | | | | | |
| Rh | | | | | | | | | | | | | | |
| Pd ppb | | | | | | | | | | | | | | |
| Ag ppb | | | | | | | | | | | | | | |
| Cd ppb | | | | | | | | | | | | | | |
| In ppb | | | | | | | | | | | | | | |
| Sn ppb | | | | | | | | | | | | | | |
| Sb ppb | | | | | | | | | | | | | | |
| Te ppb | | | | | | | | | | | | | | |
| Cs ppm | | | | | | | | | | | | | | |
| Ba | 200 | | | | | | | | | | | | | |
| La | 12.9 | | | | | | | | | | | | | |
| Ce | 30.3 | | | | | | | | | | | | | |

| | |
|----|------|
| Pr | |
| Nd | 20.4 |
| Sm | 6.31 |
| Eu | 1.18 |
| Gd | |
| Tb | 1.22 |
| Dy | |
| Ho | |
| Er | |
| Tm | |
| Yb | 3.35 |
| Lu | 0.51 |
| Hf | 2.64 |
| Ta | 0.71 |

W ppb

Re ppb

Os ppb

Ir ppb

Pt ppb

Au ppb

Th ppm 0.9

U ppm

technique (a) ICP-AES, (b) ICP-MS, (c) IDMS, (d) EMPA, (e) INAA, (f) XRF, (g) AA

References: 1) Anand et al. (2003); Demidova et al. (2003)

K. Righter, Lunar Meteorite Compendium, 2010